pH-Responsive Layered Hydrogel Microcapsules as Gold Nanoreactors

Veronika Kozlovskaya,[†] Eugenia Kharlampieva,[†] Sehoon Chang,[‡] Rachel Muhlbauer,[†] and Vladimir V. Tsukruk*[,†,‡]

School of Materials Science and Engineering, and School of Polymer, Textile and Fiber Engineering, Georgia Institute of Technology, Atlanta, Georgia 30332

Received February 3, 2009. Revised Manuscript Received April 2, 2009

We demonstrate that layered hydrogel poly(methacrylic acid) capsules (PMAA), produced from hydrogen-bonded (PMAA/poly-*N*-vinylpyrrolidone) (PMAA/PVPON) multilayer precursors through cross-linking with ethylenediamine (EDA), can facilitate in situ synthesis of gold nanoparticles within hydrogel walls under ambient conditions. The necessary amine groups are available within the (PMAA) shells due to one-end attached cross-linker molecules. We also show that the nanoparticle size can be controlled through changing the pH-dependent balance of amine/ammonium groups in the ionic cross-links within the shells. Importantly, the pH-responsive properties of the ultrathin hydrogel shells are preserved after gold nanoparticle synthesis within the capsule walls. The reported in situ synthesis of gold nanoparticles within the ultrathin and pH-responsive shells can find a potential use for straightforward and facile fabrication of the hybrid organic−gold nanomaterials for biochemical sensing and delivery applications.

Introduction

In past years, the research on metal nanoparticles as reenforcing, functional, and responsive blocks for hybrid organic/nanocomposite materials has gained significant attention due to the unique optical, electrical, catalytic, and antibacterial properties of inorganic nanoparticles.[1−4] Different inorganic materials such as silica nanoparticles, magnetite nanocrystals, metal nanoparticles, and semiconducting nanowires have been deposited onto or within polymer matrices to enhance their mechanical and optical properties.[5−7] Inclusion of metal nanoparticles within polymer materials was shown to be an effective way for a combination of unique optical properties of gold nanostructures with responsive behavior of ultrathin membranes enhancing their function as easily handable adaptive nanomaterials.[8] Such a combination allowed a robust control over various important properties of the responsive polymer films[9] such as microroughness,[10,11] wettability,[12] biocompatibility,[13] and optical response,[14] which are important for a variety of fields in separation,[15] sensing,[16,17] and delivery of functional molecules.[18]

Various methods have been used for embedding gold nanoparticles within the polymer matrix including Langmuir−Blodgett (LB) deposition,[19,20] electrostatic-driven adsorption,[21−24] and hydrogen-bonded assembly.[25] The layer-by-layer assembly (LbL) of polyelectrolyte structures on sacrificial substrates has been widely used to fabricate free-standing planar polymer films with inorganic particles for the improvement of their mechanical, delivery, and optical properties.[26−29] Polyelectrolyte capsules with nanocomposite organic/inorganic shells with embedded nanoparticles have demonstrated significant mechanical rigidity and maintain

* To whom correspondence should be addressed. E-mail: vladimir@mse.gatech.edu.
[†] School of Materials Science and Engineering.
[‡] School of Polymer, Textile and Fiber Engineering.

(1) Hu, M.; Chen, J.; Li, Z.; Au, L.; Hartland, G. V.; Li, X.; Marqueze, M.; Xia, Y. *Chem. Soc. Rev.* **2006**, *35*, 1084.
(2) Hodes, G. *Adv. Mater.* **2007**, *19*, 639.
(3) Seregina, M.; Bronstein, L.; Platonova, O.; Chernyshov, D.; Valetsky, P.; Hartmann, J.; Wenz, E.; Antonietti, M. *Chem. Mater.* **1997**, *9*, 923.
(4) Lee, D.; Cohen, R. E.; Rubner, M. F. *Langmuir* **2005**, *21*, 9651.
(5) Grigoriev, D.; Gorin, D.; Sukhorukov, G. B.; Yaschenok, A.; Maltseva, E.; Möhwald, H. *Langmuir* **2007**, *23*, 12388.
(6) Markutsya, S.; Jiang, C.; Pikus, Y.; Tsukruk, V. V. *Adv. Funct. Mater.* **2005**, *15*, 771.
(7) Gunawidjaja, R.; Jiang, C.; Peleshanko, S.; Ornatska, M.; Singamaneni, S.; Tsukruk, V. V. *Adv. Funct. Mater.* **2006**, *16*, 2024.
(8) Jiang, C.; Tsukruk, V. V. *Soft Matter* **2005**, *1*, 334.
(9) Luzinov, I.; Minko, S.; Tsukruk, V. V. *Prog. Polym. Sci.* **2004**, *29*, 635.
(10) Lupitskyy, R.; Roiter, Y.; Tsitsilianis, C.; Minko, S. *Langmuir* **2005**, *21*, 8591.
(11) Sidorenko, A.; Krupenkin, T.; Taylor, A.; Fratzl, P.; Aizenberg, J. *Science* **2007**, *315*, 487.
(12) Sidorenko, A.; Krupenkin, T.; Aizenberg, J. *J. Mater. Chem.* **2008**, *18*, 3841.
(13) Krsko, P.; Libera, M. *Mater. Today* **2005**, *8*, 36, and references therein.
(14) Houbenov, N.; Minko, S.; Stamm, M. *Macromolecules* **2003**, *36*, 5897.
(15) Bruening, M. L.; Dotzauer, D. M.; Jain, P.; Ouyang, L.; Baker, G. L. *Langmuir* **2008**, *24*, 7663.
(16) Caruso, F.; Spasova, M.; Susha, A.; Giersig, M.; Caruso, R. A. *Chem. Mater.* **2001**, *13*, 109.
(17) Cameron, A.; Shakesheff, K. M. *Adv. Mater.* **2006**, *18*, 3321.
(18) Ganta, S.; Devalapally, H.; Shahiwala, A.; Amiji, M. *J. Controlled Release* **2008**, *126*, 187.
(19) Chen, S. *Langmuir* **2001**, *17*, 2878.
(20) Endo, H.; Mitsuishi, M.; Miyashita, T. *J. Mater. Chem.* **2008**, *18*, 1302.
(21) Jiang, C. Y.; Markutsya, S.; Shulha, S.; Tsukruk, V. V. *Adv. Mater.* **2005**, *17*, 1669.
(22) Malikova, N.; Pastoriza-Santos, L.; Schierhorn, M.; Kotov, N. A.; Liz-Marzan, L. M. *Langmuir* **2002**, *18*, 3694.
(23) Dong, W. F.; Sukhorukov, G. B.; Möhwald, H. *Phys. Chem. Chem. Phys.* **2003**, *5*, 3003.
(24) Cho, J. H.; Caruso, F. *Chem. Mater.* **2005**, *17*, 4547.
(25) Hao, E.; Lian, T. *Chem. Mater.* **2000**, *12*, 3392.

10.1021/cm900314p CCC: $40.75
Published on Web 04/27/2009

their spherical shape after drying with retaining encapsulated materials in their interiors.[30,31] Usually, the encapsulation of nanoparticles requires premodification with stabilizing and capping agents when used for adsorbing onto/into multilayer films to support strong noncovalent interactions with polymer matrices during the LbL assembly.[32,33]

For instance, the "breathing strategy" was suggested for the preparation of temperature-responsive Au/poly(*N*-isopropylacrylamide) (PNIPAM) composites when gold nanoparticles were incorporated into the highly swollen gel in aqueous solution, which was later shrunk in aprotic solution to fix gold nanoparticles in the hydrogel by physical entanglement (breathing out).[34] Recently, we have reported on the preparation of (PMAA/gold nanorods) composite multilayered hydrogels through electrostatic inclusion of the CTAB-stabilized Au nanorods within the swollen multilayer hydrogel to produce pH-responsive optical materials.[35] Along with the pH-dependent shift of the surface plasmon resonance (SPR) signal, such inclusion of the gold nanorods rendered these films mechanically stable and capable of sustaining release process in free-floating state. A variety of strategies for fabrication of robust free-standing microstructures from LbL-derived materials have been summarized in our recent review.[36]

The LbL assembled polyelectrolyte capsules have been employed as microreactors for in situ synthesis of nickel−metallized poly(allylamine hydrochloride/poly(styrene sulfonate) (PAH/PSS) shells.[37] Indeed, in situ nanoparticle synthesis within the multilayer polymer films can be an elegant way to obtain metal nanoparticles and corresponding hybrid nanomaterials (organic−inorganic) due to the confined environment of the polyelectrolyte multilayers allowing a good control over nanoparticle shapes, morphologies, and sizes.[38,39] Remarkably, noble nanoparticles, gold in particular, possess good biocompatibility and nontoxicity. Various antibodies and proteins can be readily conjugated to gold nanoparticles through thiol-surface chemistry or electrostatic binding, which makes them important for biochemical sensing and detection[40] as well as for therapeutic applications.[41] Drastic temperature change of gold nanoparticles on resonance with an excitation source[42] can be used for delivery of microcapsule inner contents. Mostly, the strategy of nanoparticle synthesis within the LbL films is based on pH-dependent properties of the multilayer films assembled from weak polyelectrolytes, generally containing carboxylic acid groups, which provide binding sites for metal precursor ions under specific pH conditions.[39,43]

However, such an approach cannot be used for the direct synthesis of gold nanoparticles inside a polymer matrix because of the same electrostatic charge of negatively charged carboxylate groups and chloroaurate ions as gold precursors. Indeed, the incorporation of free amine groups useful as binding sites for gold anions within the multilayer films is a tricky challenge. On one hand, the favorable presence of free amine groups necessary for gold stabilization can be impaired by limited solubility of PAH (or poly(ethyleneimine) (PEI) at high pH conditions. On the other hand, the charge-to-charge compensation mechanism of the electrostatic LbL results in almost all ammonium groups bound to anionic counterparts under lower pH deposition conditions. Recently, Chia et al. have demonstrated the possibility of induced postassembly molecular rearrangements within PAH/PAA and PAH/PSS multilayers, which could favor gold nanoparticle synthesis within these films.[44] However, such rearrangements are limited and only possible for the (PAH/PAA) and (PAH/PSS) multilayers deposited under very specific conditions, which, to a great extent, impair both the film integrity and the robustness of nanocomposite materials.[44]

In this work, we demonstrate that multilayered hydrogel PMAA capsules, produced from hydrogen-bonded (PMAA/PVPON) multilayer LbL precursors through cross-linking with EDA, can be utilized to facilitate in situ synthesis of gold nanoparticles inside hydrogel shells. The amine groups are readily available within the (PMAA) multilayer hydrogels due to some one-end attached cross-linker molecules. In contrast to the previously reported synthesis of gold nanoparticles in polyelectrolyte multilayers discussed above, these LbL hydrogels introduced here do not require any specific pretreatment such as group activation or adding an extra component. Moreover, using this approach, the gold nanoparticle synthesis can be carried out under mild reducing conditions of borate buffer at ambient environment.

In addition, the important feature of the resulted composite shells is their pH-dependent properties, which are barely affected by the presence of synthesized gold nanoparticles. We also show how the dimension of gold nanoparticles can be controlled through the pH-dependent release of amine groups from ionic cross-links within the hollow hydrogel shells without any damage to the film, which can be a limitation for the LbL multilayers when one needs to use specific conditions of the multilayer preassembly to provide the amine groups. We suggest that in situ synthesis of gold

(26) Jiang, C. Y.; Markutsya, S.; Pikus, Y.; Tsukruk, V. V. *Nat. Mater.* **2004**, *3*, 721.
(27) Lutkenhaus, J. L.; Hrabak, K. D.; McEnnis, K.; Hammond, P. T. *J. Am. Chem. Soc.* **2005**, *127*, 17228.
(28) Mamedov, A. A.; Kotov, N. A.; Prato, M.; Guldi, D. M.; Wicksted, J. P.; Hirsh, A. *Nat. Mater.* **2002**, *1*, 190.
(29) Tang, Z. Y.; Kotov, N. A.; Magonov, S.; Ozturk, B. *Nat. Mater.* **2003**, *2*, 413.
(30) Schukin, D. G.; Sukhorukov, G. B. *Adv. Mater.* **2004**, *16*, 671.
(31) Dubreuil, F.; Schukin, D. G.; Sukhorukov, G. B.; Fery, A. *Macromol. Rapid Commun.* **2004**, *25*, 1078.
(32) *Multilayer Thin Films*; Decher, G., Schlenoff, J. B., Eds.; Wiley-VCH: Weinheim, 2003.
(33) Lvov, Y.; Decher, G.; Möhwald, H. *Langmuir* **1993**, *9*, 481.
(34) Pardo-Yissar, V.; Gabai, R.; Shipway, A. N.; Bourenko, T.; Willner, I. *Adv. Mater.* **2001**, *13*, 1320.
(35) Kozlovskaya, V.; Kharlampieva, E.; Khanal, B. P.; Manna, P.; Zubarev, E. R.; Tsukruk, V. V. *Chem. Mater.* **2008**, *20*, 7474.
(36) Jiang, C.; Tsukruk, V. V. *Adv. Mater.* **2006**, *18*, 829.
(37) Schukin, D. G.; Ustinovich, E. A.; Sukhorukov, G. B.; Möhwald, H.; Sviridov, D. V. *Adv. Mater.* **2005**, *17*, 468.
(38) Wang, T. C.; Rubner, M. F.; Cohen, R. E. *Langmuir* **2002**, *18*, 3370.
(39) Lee, D.; Rubner, M. F.; Cohen, R. E. *Chem. Mater.* **2005**, *17*, 1099.
(40) Riboh, J. C.; Haes, A. J.; McFarland, A. D.; Ranjit, C.; Van Duyne, R. P. *J. Phys. Chem. B* **2003**, *107*, 1772.
(41) El-Sayed, I. H.; Huang, X.; El-Sayed, M. A. *Cancer Lett.* **2006**, *239*, 129.
(42) Petrova, H.; Hu, M.; Hartland, G. V. *Z. Phys. Chem.* **2007**, *221*, 361.
(43) Kane, R. S.; Cohen, R. E.; Silbey, R. *Chem. Mater.* **1999**, *11*, 90.
(44) Chia, K.-K.; Cohen, R. E.; Rubner, M. F. *Chem. Mater.* **2008**, *20*, 6756.

nanoparticles within the EDA−(PMAA) LbL hydrogel capsule walls has a potential to regulate mechanical properties of the ultrathin and pH-responsive multilayer hydrogels for shape re-enforcement of three-dimensional shape-persistent and robust microstructures made of such nanostructured hybrid materials.

Experimental Section

Materials. PMAA (M_w = 150 kDa), PVPON (M_w = 55 kDa), PAH (M_w = 70 kDa), mono- and dibasic sodium phosphate 1-ethyl-3-(3-dimethylaminopropyl) carbodiimide hydrochloride (EDC), *N*-hydroxy-sulfosuccinimide sodium salt (NSS), adipic acid dihydrazide (AAD), EDA, and $HAuCl_4$ solution were purchased from Sigma-Aldrich. 0.1 M borate buffers (pH 10) were received from J. T. Baker. Monodisperse silica particles with diameter of 4.0 ± 0.2 mm were obtained from Polysciences Inc. as 10% dispersions in water. Hydrofluoric acid (48−51%) was purchased from BDH Aristar. Ultrapure (Nanopure system) filtered water with a resistivity of 18.2 MΩ cm was used in all experiments. Quartz microscope fused slides (Alfa Aesar) and single-side polished silicon wafers of the (100) orientation (Semiconductor Processing Co.) were cut by typical size of 10 × 20 mm and cleaned in a piranha solution as described elsewhere.[45]

Fabrication of Hydrogel PMAA Capsules and Films. Deposition of hydrogen-bonded multilayers of PVPON/PMAA on particulate substrates has been described previously.[46] Briefly, 0.2 mg/mL polymer solutions were used with a typical deposition time of 15 min. Hydrogen-bonded multilayers were deposited directly onto silica microparticles at pH 2.5 starting from PVPON. Each deposition cycle was followed by washing three times with a water solution with pH adjusted to 2.5. Suspensions were settled by centrifugation at 2000 rpm for 2 min to remove the supernatant with excess of polymer. Deposition, washing, and redispersion steps were performed on a VWR analogue vortex mixer at 2000 rpm. When a desired number of layers was deposited, cross-linking was performed as described earlier,[47] where the procedure consisted of activation of the carboxylic groups with 5 mg/mL solution of EDC and NSS at pH 5 followed by reaction with a 5 mg/mL solution of EDA at pH 5.8, or with 2 mg/mL solution of AAD at pH 5 for 24 h to introduce amide linkages between EDA (or AAD) molecules and the activated carboxylic groups.

In the case of quartz-tethered PMAA films, three bilayers of PAH/PMAA precursors were first spin-cast onto the quartz slides starting from 0.5 mg/mL PAH solution at pH 4 with the following deposition of PMAA from 0.5 mg/mL aqueous solution at pH 5, to enhance the surface adhesion of the subsequently grown multilayer as well as the swollen hydrogel films in borate buffers of pH 10. The precursor layers were heated to 175 °C for 1 h in an oven for thermal cross-linking of $(PAH/PMAA)_3$ layers[48] and their enhanced adhesion to the substrate surfaces. We utilized these precursor-treated quartz microslides or silicon wafers for further deposition of hydrogen-bonded (PVPON/PMAA) multilayers. Specifically, 1.0 mg/mL polymer solutions were placed onto the substrates and rotated at 4000 rpm for approximately 20 s starting from PVPON when the pretreated substrates were employed. After the desired number of bilayers was spin-LbL assembled,[49] the quartz-attached PVPON/PMAA multilayers were cross-linked as described above.

After cross-linking was completed, the particle suspensions were washed several times with the appropriate buffer solutions and exposed to pH 8 for 6 h to swell the cross-linked shell around the cores. When hollow shells were needed for analysis, the silica cores were dissolved by shaking the particle dispersion for 4 h in 8% aqueous HF solution, yielding LbL-derived hydrogel hollow capsules. The dispersion of the capsules with cross-linked capsule walls was then dialyzed against water for 2 days. The substrates with tethered hydrogel films were immersed in a 0.01 M buffer solution at pH 8 for 1 h to ensure release of PVPON and then transferred to pH 5 to deswell the hydrogel films. After 4 h of exposure, these films were dried with a gentle flow of nitrogen.

Growth of Gold Nanoparticles within Hydrogel PMAA Capsules and Films. For growth of gold nanoparticles within the hydrogel shells, suspensions of silica cores with the cross-linked hydrogel shells were washed with the borate buffers at pH 3, pH 5, or pH 10 four times and were exposed to 2 mL of 1.6 mM $HAuCl_4$ solution in 0.1 M borate buffer for 48 h in the dark. After that, the suspensions were extensively washed with the buffers with the appropriate pH values and then with water. Quartz-attached films were treated in similar way.

UV−Visible Spectroscopy (UV−vis). UV−visible spectra of hydrogel LbL films and hollow shells solutions were recorded using a UV-2450 spectrophotometer (Shimadzu). Measurements were done on quartz substrates. UV−visible spectroscopy of hollow hydrogel capsules suspensions was performed in a quartz cell with 10 mm optical path. For that, 2 mL of capsule suspensions was placed in the cell, covered with a cap, and tested.

Atomic Force Microscopy (AFM). Surface morphology of the hollow capsules and films was examined using atomic force microscopy (AFM). AFM images were collected using a Dimension-3000 (Digital Instruments) microscope in the "light" tapping mode according to the well-established procedure.[50] For capsule sample preparation, a drop of capsule suspension was placed onto a precleaned silicon wafer and dried in air prior to AFM imaging. For film thickness measurements, the capsule single wall thickness was determined as half of the height of the collapsed flat regions of dried capsules bearing analysis from NanoScope software to generate height histograms.

Transmission Electron Microscopy (TEM). TEM was performed on a JEOL 100CX-2 electron microscope operated at 100 kV. To analyze the pristine and/or nanoparticle-containing hydrogel capsules, they were placed on a carbon-coated gold grid (Electron Microscopy Sciences) and dried in air before TEM analysis.

ζ-Potential Measurements. The ζ-potentials of EDA- or AAD-cross-linked $(PMAA)_{15}$ capsules were measured at different pH values on Zetasizer Nano-ZS equipment (Malvern). The pH values of aqueous capsule solutions were adjusted using 0.01 M HCl or NaOH solutions. Each value was obtained by averaging three independent measurements.

Optical Microscopy. Optical microscopy images of EDA−$(PMAA-Au)_{15}$ capsules in solutions with various pH values were obtained at 40× in transmission mode using a Zeiss Axiovert 200 (Zeiss, Thornwood, NY) and a CCD camera. The procedure included the addition of a drop of a dispersion of the capsules to the Laboratory-Tek chambered cells (Electron Microscopy Sciences). The chambers of the Laboratory-Tek coverglass were then

(45) Zimnitsky, D.; Jiang, C.; Xu, J.; Lin, Z.; Tsukruk, V. V. *Langmuir* **2007**, *23*, 4509.
(46) Kozlovskaya, V.; Sukhishvili, S. A. *Macromolecules* **2006**, *39*, 6191.
(47) Kozlovskaya, V.; Shamaev, A.; Sukhishvili, S. A. *Soft Matter* **2008**, *4*, 1499.
(48) Yang, S. Y.; Rubner, M. F. *J. Am. Chem. Soc.* **2002**, *124*, 2100.
(49) Cho, J.; Char, K.; Hong, J.; Lee, K. *Adv. Mater.* **2001**, *13*, 1076.
(50) Tsukruk, V. V.; Reneker, D. H. *Polymer* **1995**, *36*, 1791.

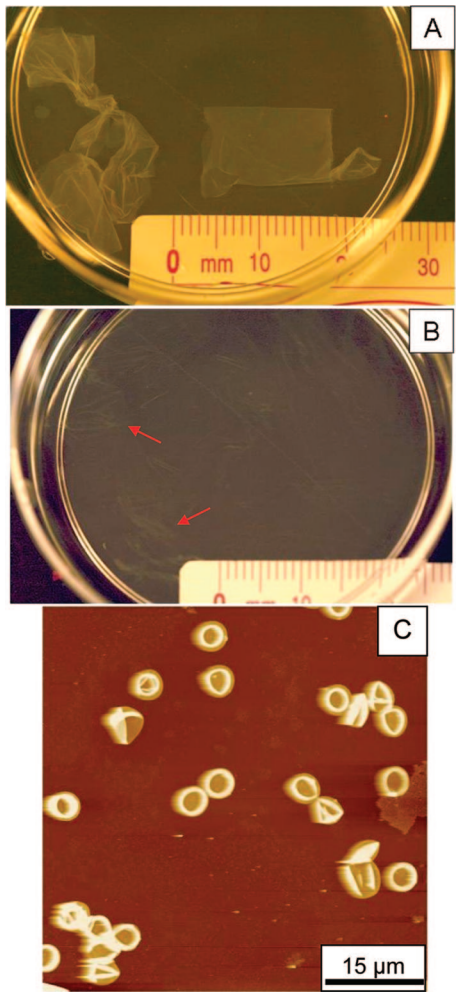

Figure 1. Optical images of freely floating $(PMAA)_{40}$ hydrogel films at pH 5 ($n = 1.43$) (A) and at pH 10 ($n = 1.36$) (B). The arrows show the edges of the swollen PMAA film. AFM image of EDA−$(PMAA)_{15}$ hollow capsules dried on a Si wafer (C); the z-scale of the image is 400 nm.

sequentially filled with buffer solutions at a certain pH. Capsules were allowed to settle and then analyzed.

Results and Discussion

Synthesis of Gold Nanoparticles within Amphoteric Hydrogels. In our previous work, we have demonstrated that multilayer-derived hydrogels produced through a cross-linking of solely poly(carboxylic acid) within the hydrogen-bonded multilayers result in amphoteric pH-dependent behavior of such films.[46] They exhibit large swelling at both high and low pH values due to ionization of either carboxylic groups (from pH 6 to pH 8) or the release of ammonium groups from the one-end attached EDA cross-linker molecules upon protonation of the carboxylic groups at pH < 4. Additionally, these multilayer-derived hydrogels swell in the pH range from 10 to 12 due to a deprotonation of ammonium groups ($pK_a \approx 10$).[51]

Figure 1 demonstrates optical images of freely floating 110 nm thick hydrogel films of $(PMAA)_{40}$ in aqueous media of different pH values. It is interesting to note that, while visible at pH 5 due to its higher refractive index of 1.43

Scheme 1. Schematic Representation of Ultrathin Nanocomposite $(PMAA/Au)_n$ Hydrogel Membrane Construction at Surfaces[a]

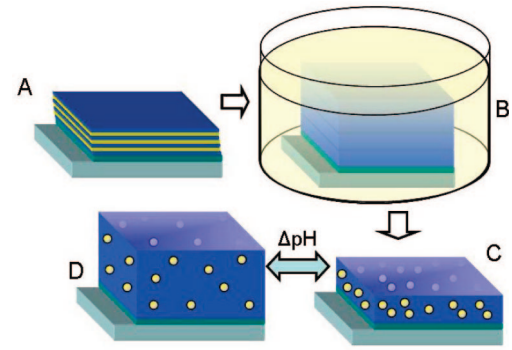

[a] (A) The LbL assembly of hydrogen-bonded $(PVPON/PMAA)_n$ films that are chemically cross-linked with EDA. (B) Swollen $(PMAA)_n$ hydrogel is incubated in chloroaurate solution in borate buffer at pH 10. (C,D) Deswollen and swollen surface-attached nanocomposite $(PMAA-Au)_n$ hydrogel membranes.

(Figure 1A), the film becomes almost invisible in solution at pH 10 (Figure 1B), where its refractive index decreases to 1.36 due to the large degree of swelling of the hydrogel.[52] The large degree of softness of such responsive membranes is further illustrated in Figure 1C. These swollen films produced as closed hollow membranes (microcapsules) exhibit a distinctive drying behavior. As seen from the low-magnification height AFM image, up to 70% of the swollen PMAA capsules dried from aqueous solution at pH 7 collapsed with the large unfolded adhesion area, yielding almost perfectly round dried capsules. Such drying behavior of the capsules reflects drastic softening of the capsule walls with the microcapsule stiffness decrease by a factor of 600 with the value as low as 1 mN/m as determined by single-capsule AFM measurements.[53]

As cross-linked with EDA, such ultrathin LbL-derived hydrogel films possess groups of the opposite charge, free amine groups within the cross-linked matrix of the poly(methacrylic acid) chains. Previously, it has been shown that these oppositely charged functionalities can be used to control the permeability of these membranes toward low and high molecular weight compounds and the adhesion properties of the hollow shells at surfaces of a different surface charge.[46,54] Initially, to investigate the ability of these hydrogels to serve as nanoreactors for the synthesis of gold nanoparticles due to the present amine groups, surface-tethered hydrogel $(PMAA)_{10}$ films were constructed on quartz slides using the spin-assisted LbL assembly of hydrogen-bonded $(PVPON/PMAA)_{10}$ films.[35]

Scheme 1 shows the pathway for the synthesis of gold nanoparticles within the pH-responsive $(PMAA)_n$ hydrogels exploiting free amine groups. First, hydrogen-bonded multilayers of $(PVPON/PMAA)_{10}$ were built using the SA-LbL

(51) Albert, A.; Serjeant, E. P. *Ionization Constants of Acids and Bases*; J. Wiley and Sons: New York, 1962.
(52) Pristinski, D.; Kozlovskaya, V.; Sukhishvili, S. A. *J. Opt. Soc. Am. A* **2006**, *23*, 2639.
(53) Elsner, N.; Kozlovskaya, V.; Sukhishvili, S. A.; Fery, A. *Soft Matter* **2006**, *2*, 966.
(54) Kharlampieva, E.; Erel-Unal, I.; Sukhishvili, S. A. *Langmuir* **2007**, *23*, 175.

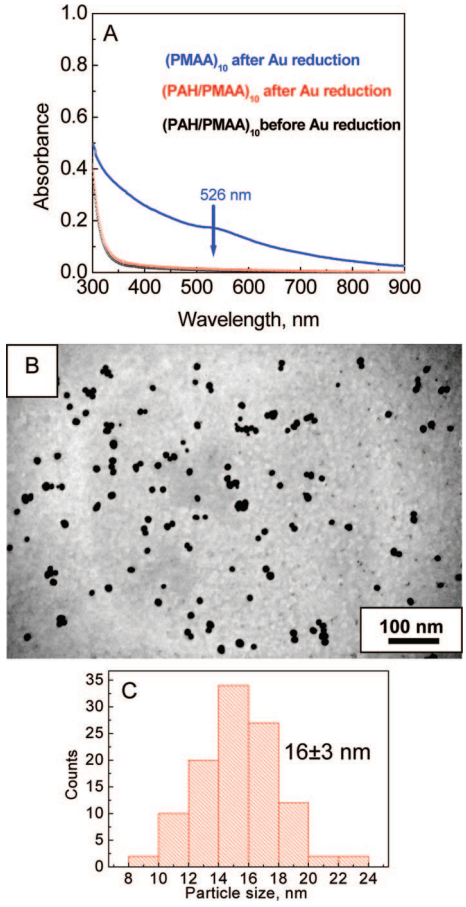

Figure 2. (A) UV−visible spectra of quartz-tethered-thermally cross-linked $(PAH/PMAA)_{10}$ and EDA−$(PMAA)_{10}$ films (red and blue, respectively) after gold reduction in borate buffer at pH 10 for 2 days. The spectrum of thermally cross-linked $(PAH/PMAA)_{10}$ before Au reduction is shown in black for reference. TEM images of quartz-attached-$(PMAA)_{20}$ hydrogel films with gold nanoparticles reduced at pH 10 in borate (B) buffers with size distributions of the nanoparticles (C).

method (Scheme 1A) and later cross-linked with EDA, producing $(PMAA)_{10}$ ultrathin hydrogel-like films. To ensure robust attachment of the pH-responsive LbL-derived hydrogel to a quartz support, $(PVPON/PMAA)_{10}$ films were deposited on $(PAH/PMAA)_2$-thermally cross-linked prelayers. This approach allows for the formation of the reliable anchoring layer between the solid support and the LbL hydrogel film.[55] Next, the swollen LbL $(PMAA)_{10}$ hydrogel was exposed to chloroaurate acid solution in borate buffer at pH 10 to facilitate gold reduction (Scheme 1B).

The UV−visible spectrum of the quartz-attached $(PAH/PMAA)_2(PMAA)_{10}$ film after gold reduction in borate buffer at pH 10 shows an absorbance peak around 526 nm corresponding to the SPR of gold nanoparticles with the diameter below 50 nm[56] (Figure 2A). It is important to note that the control films of thermally cross-linked $(PAH/PMAA)_{10}$ did not reduce gold under mild reducing conditions of borate buffer[57] used for the reaction. As seen from Figure 2A, the UV−visible spectra of the thermally cross-linked $(PAH/PMAA)_{10}$ films before (black) and after (red) exposure

(55) Kozlovskaya, V.; Kharlampieva, E.; Mansfield, M. L.; Sukhishvili, S. A. *Chem. Mater.* **2006**, *18*, 328.
(56) Wang, B.; Chen, K.; Jiang, S.; Reincke, F.; Tong, W.; Wang, D.; Gao, C. Y. *Biomacromolecules* **2006**, *7*, 1203.

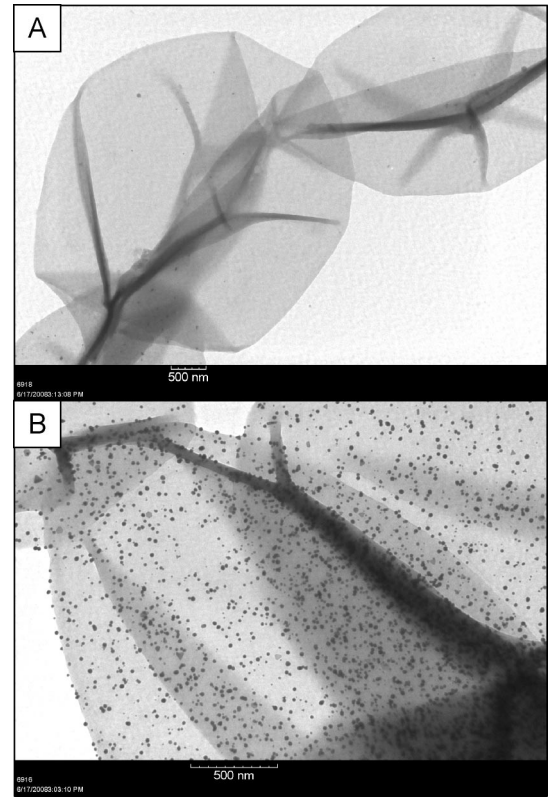

Figure 3. TEM images of AAD−$(PMAA)_{10}$ and EDA−$(PMAA)_{10}$ hollow capsules (A and B, respectively) after 48 h exposure to $HAuCl_4$ solution in borate buffer at pH 10.

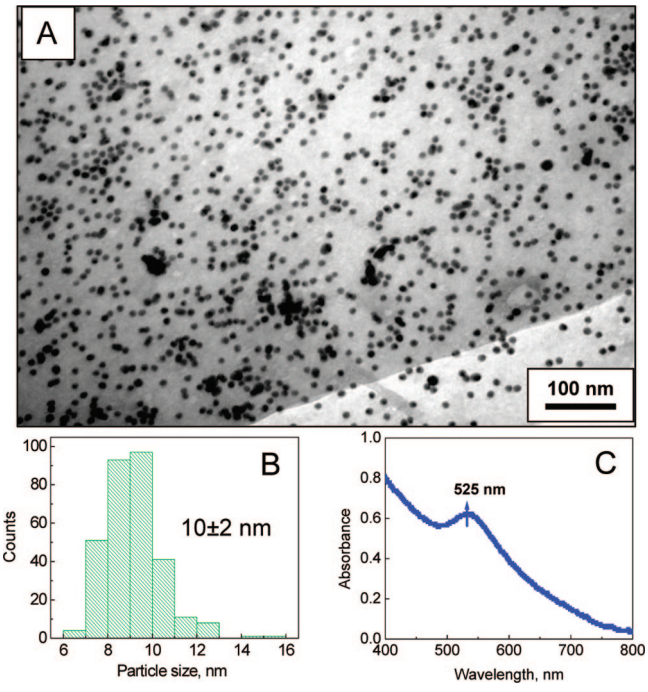

Figure 4. A higher magnification TEM image of an EDA−$(PMAA)_{15}$ capsule after 48 h exposure to $HAuCl_4$ solution in borate buffer at pH 10 (A). (B) Size distribution of the reduced gold nanoparticles. (C) A UV−visible spectrum of the EDA−$(PMAA)_{15}$ capsule solution after the gold reduction at pH 10.

to $HAuCl_4$ solution in borate buffer at pH 10 are similar. They do not show the SPR absorption band characteristic of gold, indicating no gold synthesis. These results can be explained due to the thermal cross-linking of (PAH/PMAA)

Scheme 2. Formation of Gold Nanoparticles within the (PMAA) Multilayer Hydrogels in Borate Buffer at pH 10

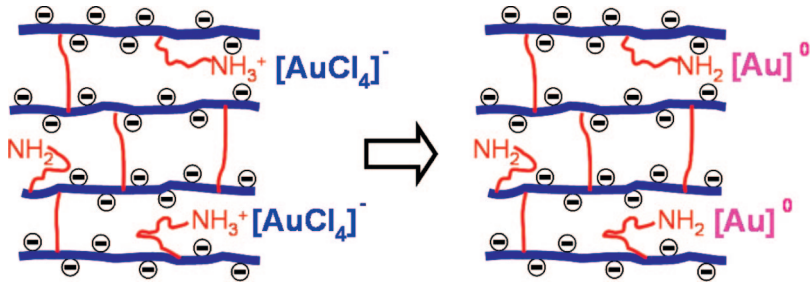

films at 175 °C for 1 h used in this work resulting in almost complete consumption of amine groups in forming amide linkages with carboxylic groups of the polyacid,[48] and therefore, no gold complex ions, $[AuCl_4]^-$, can be electrostatically retained within the film. Similar results were reported recently by Chia et al., when no detectable SPR absorption bands were found when (PAH/PAA) multilayers deposited at pH 3.5 were exposed to gold anion solutions and subsequently irradiated with UV light. This observation confirms the unsuccessful binding of the gold complex anions due to the absence of free amine/ammonium groups capable of the anion binding.[44]

TEM analysis of the $(PMAA)_{10}$ film after its exposure to $HAuCl_4$ solution in borate buffer at pH 10 revealed the presence of monodisperse gold nanoparticles with relatively narrow size distribution (below 20%) and the average size of 16 nm (Figure 2B,C). It is worth noting that if the gold reduction was performed under the same conditions except that the dibasic phosphate buffer was used, gold nanoparticles with a broad distribution of sizes and shapes were produced (not shown).

As a next step, we synthesized $(PMAA)_{10}$ hydrogel capsules using another bifunctional cross-linker, adipic acid dihydrazide, to confirm that gold nanoparticle synthesis is facilitated by the amine groups. These capsules are further denoted as AAD−$(PMAA)_{10}$ capsules. No gold nanoparticles were detected within the AAD−$(PMAA)_{10}$ capsules after exposure to $HAuCl_4$ solution at pH 10 in borate buffer as can be seen from TEM images of the dried capsules shown in Figure 3. In contrast, the TEM analysis of the EDA−$(PMAA)_{10}$ capsules treated by the chloroaurate acid solution revealed the presence of monodisperse nanoparticles of 10 ± 3 nm in diameter (Figure 4A,B). The absorbance band at 525 nm from the solution of these capsules is attributed to the gold SPR peak and confirms the synthesis of gold nanoparticles (Figure 4C).

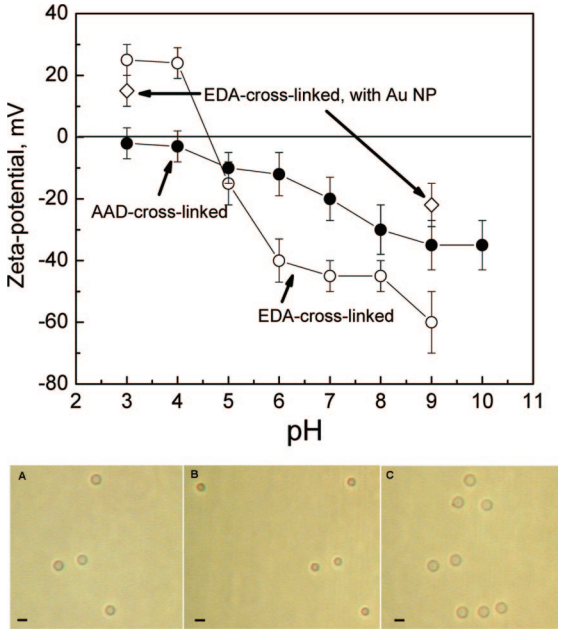

Figure 5. Top: ζ-potentials of EDA-cross-linked $(PMAA)_{15}$ (○) and AAD-cross-linked capsules (●) as a function of pH. "◇" show ζ-potential values for the EDA−$(PMAA)_{15}$ capsules containing gold nanoparticles. The pH values of aqueous capsule solutions were adjusted using HCl and NaOH solutions. Bottom: Optical microscopy images of EDA−$(PMAA-Au)_{15}$ capsules at pH = 3 (A), pH = 5 (B), and pH = 10 (C). The scale bar is 6 μm for all images.

On the basis of these findings, the suggested mechanism of the formation of gold nanoparticles is presented in Scheme 2. First, the internal structure of the EDA−(PMAA) hydrogel at pH 10 is shown in Scheme 2. At this pH, the EDA−PMAA LbL-derived hydrogel is swollen due to unscreened ionized $-COO^-$ groups and the osmotic pressure of ions. (Note that during reduction, 0.1 M borate buffer is used.) Under these conditions of high pH and partial screening of ionic $-COO^-/-NH_3^+$ cross-links, both amine and ammonium groups are present in the swollen hydrogel as the pK_b value of a primary amine is around 10. The unscreened ammonium groups become available for binding the gold anions. After the unbound gold complex ions rinsed away, the bound ones are slowly reduced under mild conditions of the borate buffer solution into gold atoms.[57]

In the case of AAD−(PMAA) shells, one-end attached AAD cross-linker molecules should not carry any positive charge at pH 10 due to their relatively low pK_b value and therefore do not bind gold complex ions, resulting in no gold nanoparticle synthesis. The presence of deprotonated amine groups within the EDA−(PMAA) hydrogel shells at pH 10 is also important for stabilization of reduced gold due to the high affinity of gold to amine groups[58,59] (Scheme 2, right). It is also worth noting that the integrity of the hydrogel film is not affected by the consumption of ammonium or amine groups during gold ions/atoms binding/stabilizing processes because of the covalent cross-links, which provide the overall pH stability of the film. Because of this, no additional precaution is needed to maintain the film integrity during

(57) Kharlampieva, E.; Slocik, J. M.; Ko, H.; Tsukruk, T.; Naik, R. R.; Tsukruk, V. V. *Chem. Mater.* **2008**, *20*, 5822.
(58) Wangoo, N.; Bhasin, K. K.; Mehta, S. K.; Raman Suri, C. *J. Colloid Interface Sci.* **2008**, *323*, 247.
(59) Kim, Y.-J.; Cho, G.; Song, J. H. *J. Nanosci. Nanotechnol.* **2006**, *6*, 3373.

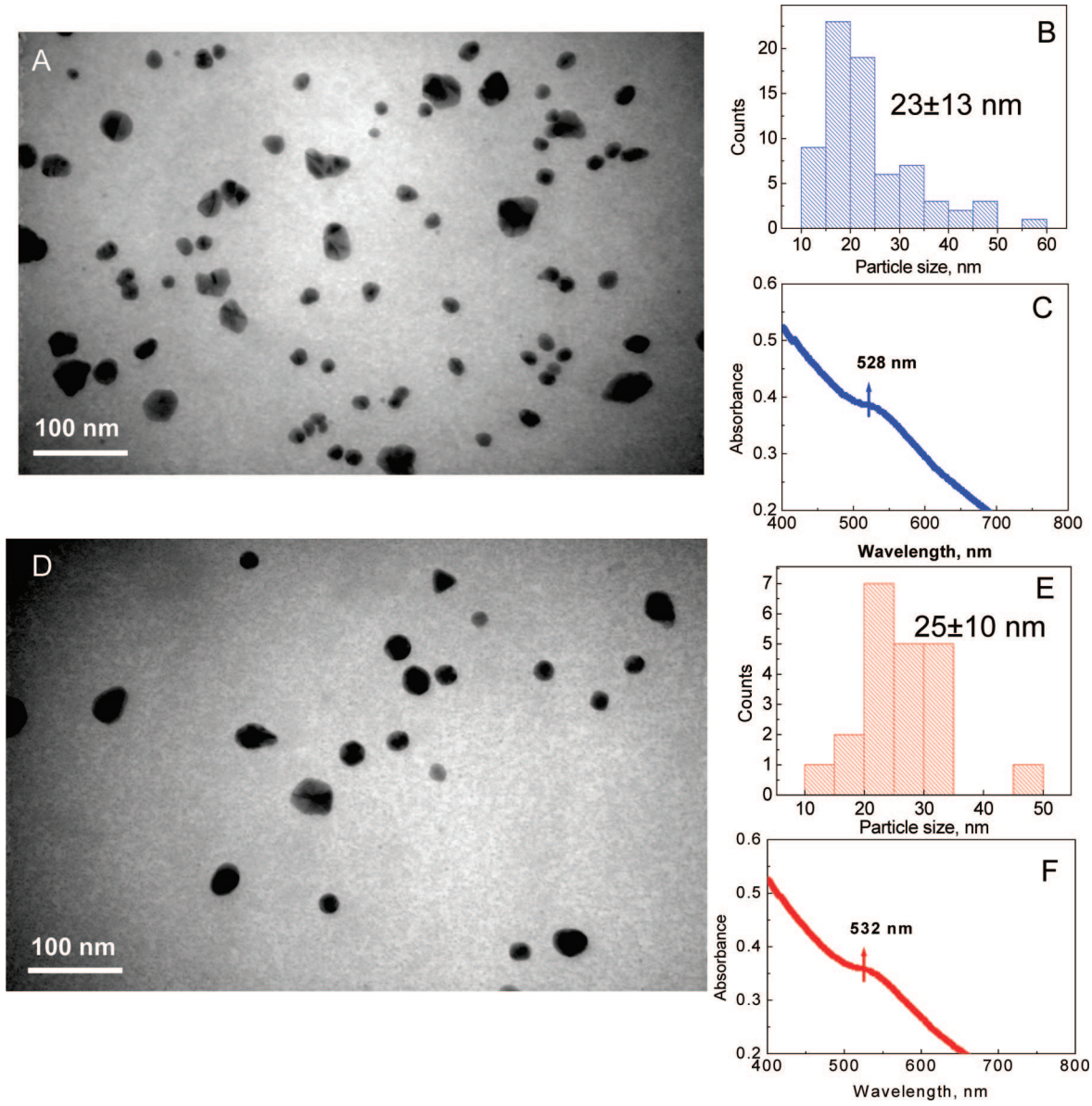

Figure 6. TEM images of EDA−$(PMAA)_{15}$ capsules after 48 h exposure to $HAuCl_4$ solution in borate buffer at pH 5 (A) and pH 3 (D) after silica cores were dissolved. The size distributions of the reduced gold nanoparticles (parts B and E: for capsules initially incubated at pH 5 and at pH 3, respectively) and UV−visible spectra of hollow capsule solutions (parts C and F: initially incubated at pH 5 and at pH 3, respectively).

such high pH conditions, which is absolutely necessary in the case of the PAH/PAA or PAH/PSS films.[44]

pH-Responsive Properties of the Hydrogel Gold-Containing EDA−(PMAA) Capsules. The important feature of the hydrogel EDA−(PMAA) LbL films and capsules is a reversible response to environmental pH changes due to carboxylic or amino functionalities.[46]To investigate the pH-dependent properties of the gold-containing hydrogel capsules synthesized here (denoted as EDA−(PMAA−Au)), ζ-potentials of the EDA−(PMAA−Au) capsule aqueous solutions were measured under various pH conditions.

Figure 5 demonstrates that when cross-linked with the different cross-linkers, EDA or AAD, $(PMAA)_{15}$ capsules exhibit the pH response in both cases. While both types of the hydrogel capsules, EDA−$(PMAA)_{15}$ and AAD−$(PMAA)_{15}$ (Figure 5, "○" and "●", respectively), possess a negative surface charge at pH > 4.5 due to ionization of the carboxylic groups,[47] almost no surface charge is observed for AAD−$(PMAA)_{15}$ capsules at pH < 4.5 unlike the EDA−$(PMAA)_{15}$ capsules. This difference is explained by the different pK_b values for the primary amine ($pK_b \approx 10$)[51] and hydrazide groups ($pK_b \approx 3$)[60] of the two cross-linkers. Because of this, while a positive surface charge at pH lower than 4.5 can be supplied by $-NH_3^+$ groups in EDA−$(PMAA)_{15}$ capsules, AAD−$(PMAA)_{15}$ capsules along with covalently two-end attached AAD-molecules, presumably, carry mostly neutral free hydrazide groups from one-end attached AAD molecules. Also, the surface charge behavior for the AAD−(PMAA) and EDA−(PMAA) hollow shells is different at pH > 8. The latter shows an additional decrease in the ζ-potential at pH > 8, which is explained by deprotonation of the primary amino groups and resultant dissociation of ionic cross-links in this pH range.[46,54]

Alternatively, the AAD−(PMAA) capsules exhibited almost no change in the ζ-potential at pH higher than 8. This observation can be again rationalized through the

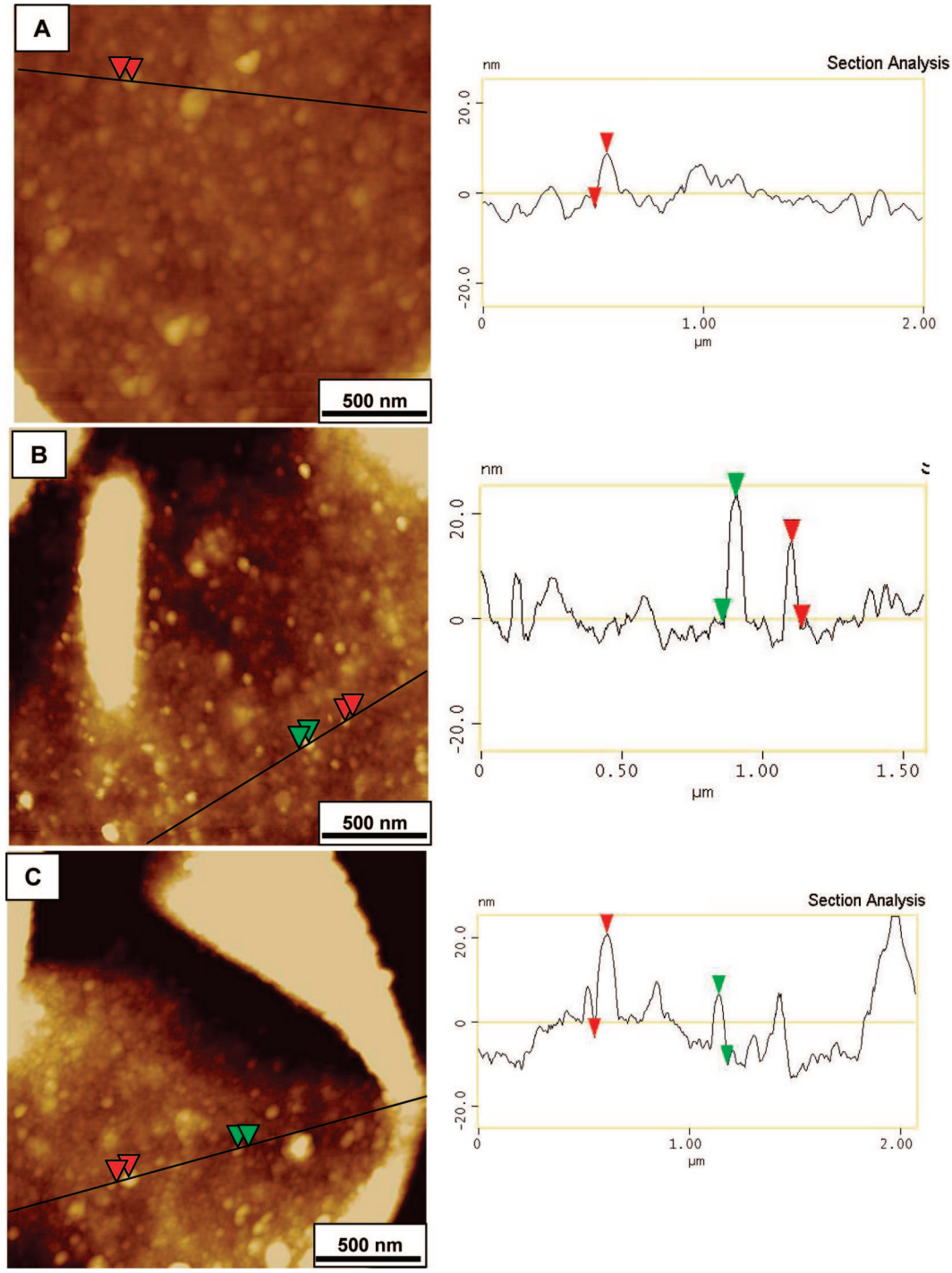

Figure 7. AFM images and corresponding cross sections of the EDA−$(PMAA)_{20}$ hollow capsules (A) with Au nanoparticles reduced in the borate buffer at pH 5 (B) and at pH 3 (C). The *z*-scale is 30 nm for all images.

large difference in pK_b values for the functional groups of the used cross-linkers; all available (not reacted) hydrazide functionalities should be already deprotonated in the AAD−(PMAA) shell at pH > 5, and the acquisition of more negative ζ-potential values is solely due to ionization of polyacid matrix. Thus, these uncharged hydrazide groups are not capable of electrostatic binding the gold complex ions and gold synthesis within AAD−$(PMAA)_{15}$ capsule walls.

After reduction of gold nanoparticles within the EDA−$(PMAA)_{15}$ capsule walls, one might expect the loss of pH-responsive properties at acidic conditions due to the consumption of free amino groups within the hydrogel shells for gold stabilization. However, the EDA−$(PMAA-Au)_{15}$ capsules exhibited the switch of the negative ζ-potential of −22 ± 7 mV to a positive value of 15 ± 5 mV when pH was changed from pH = 9 to pH = 3 (Figure 5, ◇). The optical microscopy of the EDA−$(PMAA-Au)_{15}$ capsules in different pH solutions revealed pH-dependent size changes

(60) Shafer, D. E.; Toll, B.; Schuman, R. F.; Nelson, B. L.; Mond, J. J.; Lees, A. *Vaccine* **2000**, *18*, 1273.

of the composite capsule shells (Figure 5, bottom panel). Overall, the swelling behavior of the EDA−(PMAA−Au)$_{15}$ capsules follows that of the pristine hydrogel capsules.[46] Three distinct swelling regions of EDA−(PMAA−Au)$_{15}$ capsules are clearly seen in the images. Swelling of the capsules at pH 3 (Figure 5A) and pH 10 (Figure 5C) with the respective capsule diameters of 6.2 ± 0.2 and 7.2 ± 0.3 μm is explained by the presence of $-NH_3^+$ and $-COO^-$ groups, respectively. At the intermediate pH = 5, the capsules are shrunk with the average capsule diameter of 4.0 ± 0.3 μm and become almost 2 times smaller than those at pH 10 (Figure 5B). These results clearly indicate that the EDA−(PMAA−Au)$_{15}$ shells preserved their amphoteric pH-responsive behavior after the synthesis of gold nanoparticles.

Effect of pH on Synthesis of Gold Nanoparticles. We examined the effect of the reduction pH on gold nanoparticle shape and size distribution. The hydrogel EDA−(PMAA)$_{15}$ core−shell capsules were exposed to chloroaurate acid in 0.1 M buffer solutions at pH = 5 and pH = 3 (further denoted as EDA−(PMAA−Au-5)$_{15}$ and EDA−(PMAA−Au-3)$_{15}$, respectively). After thorough rinsing with water and dissolution of the silica cores, the dialyzed capsules were subjected to TEM analysis (Figure 6).

The synthesis of gold nanoparticles under these conditions is confirmed by UV−visible spectra of the capsule solutions, which show the SPR bands at a wavelength close to 530 nm (Figure 6C,F) and from EDX analysis of the capsules (Supporting Information, Figure S1). Moreover, the gold nanoparticles synthesized within the EDA−(PMAA) hydrogel capsule walls at pH 5 and pH 3 are significantly larger than those at pH 10. They possess a broad size distribution with average diameters of 23 ± 13 nm (Figure 6A,B) and 25 ± 10 nm (Figure 6D,E), respectively.

We suggest that gold nanoparticle growth at the low pH 3 can be explained by the electrostatic binding of the precursor gold complex ions to the ammonium groups. However, the number of available ammonium groups is decreased by the presence of salt ions provided with 0.1 M borate buffer, which is known to screen electrostatic charges.[46] As a result, fewer particles are formed at pH 3 (Figure 6D). In contrast, at pH 5, the presence of salt ions (0.1 M borate buffer) results in the EDA−(PMAA) hydrogel expansion[46] due to disruption of $-COO^-/-NH_3^+$ ionic cross-links as a result of salt ion competition for binding sites. This suggestion is confirmed by TEM analysis shown in Figure 6A and D. The surface coverage is 3% and 9% for the gold reduction performed at pH = 3 and pH = 5, respectively. It is known that almost complete disruption of $-COO^-/-NH_3^+$ ionic cross-links occurs at low salt concentration of 0.04 M, suggesting the larger number of ammonium groups available for binding gold ions at pH 5 as compared to pH 3.[46]

From the cross-sectional analysis of the higher magnification AFM images shown in Figure 7, the size of the particles ranges from 19 ± 9 nm for EDA−(PMAA−Au)$_{15}$ capsules with gold synthesized at pH 5 to 26 ± 10 nm for those grown at pH 3 (Figure 7B,C). These results are similar to those obtained from TEM analysis of the EDA−(PMAA−Au-pH 5)$_{15}$ and EDA−(PMAA−Au-pH 3)$_{15}$ capsules. In comparison, the root-mean-square roughness of (1 μm × 1 μm) area of the pristine EDA−(PMAA)$_{15}$ capsules is 2.0 ± 1.0 nm, which is higher than that for the similar flat films,[35] but similar to the value of 1.9 ± 0.3 nm reported earlier for (PMAA)$_{10}$ capsules.[47] The larger nanoparticles obtained at pH 5 and pH 3 can be rationalized by the fact that, under these conditions, there are no deprotonated amine groups available within the hydrogel. Therefore, the produced nanoparticles are less stabilized than those at pH 10, which results in the observed increase in the particle size due to their aggregation. Similar trends were found in the case of the (PAH/PAA) films used for reduction of gold under UV irradiation.[44]

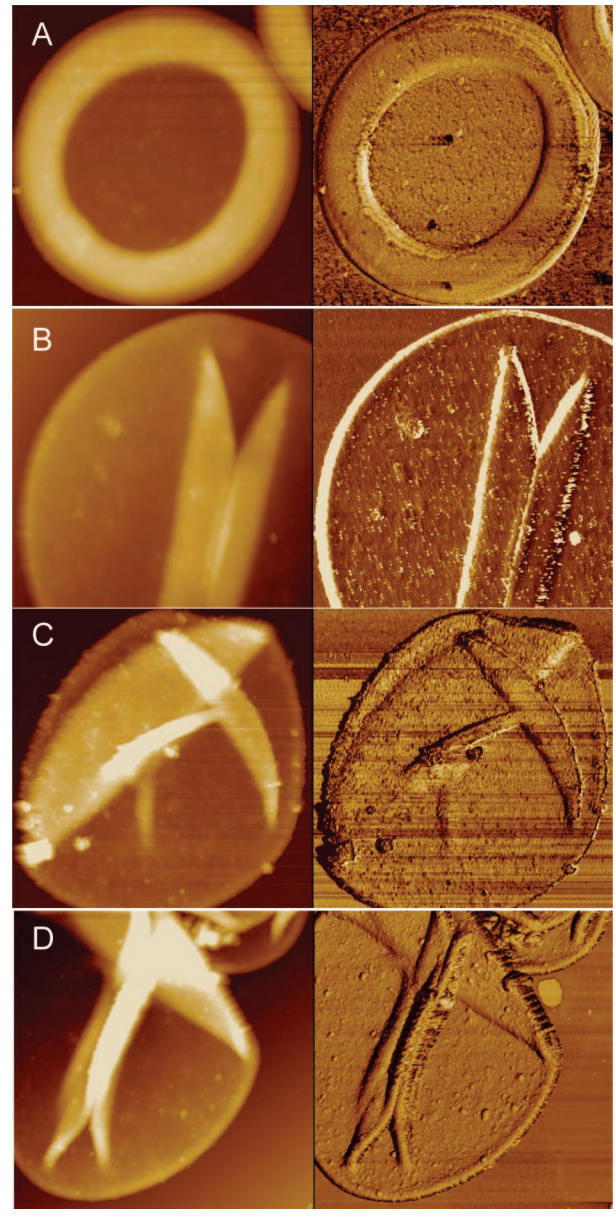

Figure 8. AFM images (height, left; phase, right) of the EDA−(PMAA)$_{15}$ hollow capsules (A) with Au nanoparticles reduced in borate buffers at pH 10 (B), pH 5 (C), and pH 3 (D). The scan size is 5 μm, and the *z*-scale is 400 nm for all images (height).

Figure 8 demonstrates the representative AFM single-capsule images of the pristine hydrogel EDA−(PMAA)$_{15}$ capsules (Figure 8A) and those with gold nanoparticles

synthesized at pH 10, pH 5, and pH 3 (Figure 8B−D, respectively). The pure hydrogel capsules demonstrate the particular folding behavior upon drying from an aqueous solution. Because of a very soft wall of the capsule at pH 7,[53] the capsule collapses uniformly without any wrinkles and with a smooth circular rim. In contrast, when the hydrogel capsule walls are re-enforced with the in situ grown gold nanoparticles, the capsule drying morphology changes dramatically. The dried capsules start forming distinctive folds, indicating changes in the mechanical properties of the composite hydrogel shells, which is highly evident from the phase images (Figure 8, right column). Multiple wrinkles are formed in central and peripheral regions of the collapsed capsules, indicating buckling instability of stiffer capsule walls with gold nanoparticles.[61]

Conclusions

In summary, we have demonstrated that LbL multilayered hydrogel PMAA hollow shells can easily facilitate direct in situ synthesis of gold nanoparticles directly within the capsule shells. In contrast to the previously reported synthesis of gold nanoparticles in polyelectrolyte multilayers, these hydrogel capsules do not require any specific pretreatment, and the particle synthesis can be carried out without any additional reducing agents in borate buffer solutions at ambient conditions. The control over gold nanoparticle size can be performed via regulating the availability of amine groups. In particular, we show that the well-dispersed gold nanoparticles of 10 ± 2 nm can be obtained within the PMAA hydrogel shells at pH 10 when free amine groups are able to stabilize reduced nanoparticles. Most importantly, the pH-responsive properties of the ultrathin (PMAA) hydrogel shells are preserved after gold nanoparticles are directly synthesized within the capsule walls in a straightforward and facile way. The dependence of the overall microcapsule stiffness on the size of the grown gold nanoparticles within the hydrogel shells will be addressed in our forthcoming studies.

Acknowledgment. This work is supported by funding provided by NSF-CBET-NIRT 0650705 grant and the AFOSR FA9550-05-1-0209 project. We are also grateful to Nils Kröger and Valeria Milam (Georgia Institute of Technology) for providing their facilities for zeta-potential measurements and optical microscopy imaging.

Supporting Information Available: Energy dispersive X-ray spectrographs (EDX) of EDA-cross-linked-$(PMAA)_{15}$ hydrogel capsules with gold reduced at pH 3 (A), at pH 5 (B), and at pH 10 (C) after cores were dissolved in HF solution and resultant hollow capsules were dialyzed (PDF). This material is available free of charge via the Internet at http://pubs.acs.org.

CM900314P

(61) Jiang, C.; Singamaneni, S.; Merrick, E.; Tsukruk, V. V. *Nano Lett.* **2006**, *6*, 2254.